Oxygen-17 NMR, Electronic, and Vibrational Spectroscopy of Transition Metal Peroxo Complexes: Correlation with Reactivity

Martha S. Reynolds*,† and Alison Butler‡

Departments of Chemistry, Colgate University, Hamilton, New York 13346, and University of California, Santa Barbara, California 93106

Received September 15, 1995⊗

The ^{17}O NMR chemical shifts of several previously characterized mono- and diperoxo complexes of vanadium(V), molybdenum(VI), tungsten(VI), and titanium(IV) were measured. Compilation of NMR, electronic, and vibrational spectroscopic data and metric parameters for these and other complexes permits us to draw correlations among ^{17}O peroxo chemical shift, the electronic charge transfer band, the O−O vibrational frequency, and the length of the oxygen−oxygen bond. Monoperoxo complexes exhibit ^{17}O chemical shifts of 500−660 ppm, while those of diperoxo complexes fall in the range 350−460 ppm. The correlation of chemical shift with the inverse ligand-to-metal charge transfer energy from electronic spectra is consistent with a formalism developed by Ramsey, despite the variations in the metals, the number of peroxo ligands, and the nature of the remaining ligands in the coordination sphere. Vibrational frequency and length of the oxygen−oxygen bond also correlate with the inverse ligand-to-metal charge transfer energy. Monoperoxo complexes show values of ν_{O-O} above 900 cm^{-1} and O−O distances in the range 1.43−1.46 Å. Diperoxo complexes have values of ν_{O-O} below 900 cm^{-1} and O−O distances of 1.46−1.53 Å. The assignment of $\nu_{O-O} = 910$ cm^{-1} for the infrared spectrum of ammonium aquaoxoperoxo(pyridine-2,6-dicarboxylato)vanadium(V), $NH_4[VO(O_2)(dipic)(H_2O)]$, was made by isotopic substitution. The stretching frequency and length of the O−O bond for peroxo complexes are explained in terms of σ-bonding between a metal d orbital and a peroxo π^* orbital. A comparison of the spectroscopic properties of these complexes with their reactivity as oxidizing agents suggests that the strength of the O−O bond is an important factor. The most reactive species exhibit λ_{max} values below 400 nm, stretching frequencies below 900 cm^{-1}, and ^{17}O chemical shifts below 600 nm. These generalizations may permit the prediction of peroxometal reactivity from spectroscopic information.

Introduction

Coordination to a metal center activates peroxide toward the oxidation of a variety of substrates, rendering peroxometal complexes important as intermediates in biological and synthetic catalysis. Peroxo complexes of iron porphyrins compose the active site of catalases and peroxidases;[1] a peroxovanadium(V) intermediate is involved in the activity of vanadium bromoperoxidase;[2] and synthetic peroxo complexes of various metals[3−5] catalyze the oxidation of arenes, alcohols, olefins, phosphines, sulfides, and halides.[6−10] In addition, several synthetic peroxovanadium(V) complexes are effective insulin mimics, presumably employing an oxidative mechanism.[11,12] The reactivity of peroxometal complexes is influenced by the identity of the metal atom, the number of peroxo ligands, and the nature of the remaining ligands in the coordination sphere. For example, oxo diperoxo aqua complexes of tungsten(VI), molybdenum(VI), and vanadium(V) oxidize a cobalt-bound thiolate ligand at rates that decrease as the metal is varied in the order listed.[13] The oxidation of bromide yields similar effects for this series[14] and for the related oxo diperoxo oxalate complexes.[15] Further, a distinction can be made between the relatively high reactivity of peroxo complexes of early transition metals in their highest oxidation states, which function as Lewis acids toward peroxide, and the low reactivity of peroxo complexes of the group VIII metals in low oxidation states, which function as Lewis bases.[7,16] Diperoxo complexes of d^0 transition metals are believed to be more reactive than their monoperoxo counterparts in some instances[13,17−19] and less reactive in others.[20−24] The effect of the chelating ligand on the reactivity of peroxo complexes is exemplified by the fact that $MoO(O_2)_2(C_2O_4)^{2-}$ oxidizes a cobalt-bound thiolate ligand[17] and bromide[15] at rates approximately 10 times faster than does $MoO(O_2)_2(OH)(H_2O)^-$. Because oxidation by peroxometal

* To whom correspondence should be addressed.
† Colgate University.
‡ University of California.
⊗ Abstract published in *Advance ACS Abstracts,* March 15, 1996.

(1) Meunier, B. In *Catalytic Oxidations with Hydrogen Peroxide as Oxidant*; Strukul, G., Ed.; Kluwer: Boston, 1992; Chapter 5, pp 153−175.
(2) Wever, R.; Krenn, B. E. In *Vanadium in Biological Systems*; Chasteen, N. D., Ed.; Kluwer: Boston, 1990; Chapter V, pp 81−97.
(3) Connor, J. A.; Ebsworth, E. A. V. *Adv. Inorg. Chem. Radiochem.* **1964**, *6*, 279−381.
(4) Dickman, M. H.; Pope, M. T. *Chem. Rev.* **1994**, *94*, 569−584.
(5) Butler, A.; Clague, M. J.; Meister, G. E. *Chem. Rev.* **1994**, *94*, 625−638.
(6) Mimoun, H. In *The Chemistry of Peroxides*; Patai, S., Ed.; Wiley: New York, 1983; Chapter 15.
(7) Sheldon, R. A.; Kochi, J. K. *Metal-Catalyzed Oxidation of Organic Compounds*; Academic: New York, 1981; Chapter 4, pp 71−119.
(8) *Catalytic Oxidations with Hydrogen Peroxide as Oxidant*; Strukul, G., Ed.; Kluwer: Boston, 1992.
(9) Kitajima, N.; Akita, M.; Moro-oka, Y. In *Organic Peroxides*; Ando, W., Ed.; Wiley: Chichester, U.K., 1992; Chapter 11.1, pp 535−558.
(10) Conte, V.; DiFuria, F.; Modena, G. In *Organic Peroxides*; Ando, W., Ed.; Wiley: Chichester, U.K., 1992; Chapter 11.2, pp 559−598.
(11) Shaver, A.; Ng, J. B.; Hall, D. A.; Lum, B. S.; Posner, B. I. *Inorg. Chem.* **1993**, *32*, 3109−3113.
(12) Posner, B. I.; Faure, R.; Burgess, J. W.; Bevan, A. P.; Lachance, D.; Zhang-Sun, G.; Fantus, I. G.; Ng, J. B.; Hall, D. A.; Lum, B. S.; Shaver, A. *J. Biol. Chem.* **1994**, *269*, 4596−4604.
(13) Ghiron, A. F.; Thompson, R. C. *Inorg. Chem.* **1990**, *29*, 4457−4461.
(14) Meister, G. E.; Butler, A. *Inorg. Chem.* **1994**, *33*, 3269−3275.
(15) Reynolds, M. S.; Morandi, S. J.; Raebiger, J. W.; Melican, S. P.; Smith, S. P. E. *Inorg. Chem.* **1994**, 33, 4977−4984.
(16) Strukul, G. In *Catalytic Oxidations with Hydrogen Peroxide as Oxidant*; Strukul, G., Ed.; Kluwer: Boston, 1992; Chapter 6, pp 177−221.
(17) Ghiron, A. F.; Thompson, R. C. *Inorg. Chem.* **1989**, *28*, 3647−3650.
(18) Abu-Omar, M. M.; Espenson, J. H. *J. Am. Chem. Soc.* **1995**, *117*, 272−280.
(19) Hansen, P. J.; Espenson, J. H. *Inorg. Chem.* **1995**, *34*, 5839−5844.

0020-1669/96/1335-2378$12.00/0

complexes is satisfactorily described in these cases by oxygen atom transfer in a mechanism involving attack of substrate on the peroxo ligand,[10,17,25,26] we seek to identify those structural and electronic properties of the peroxo ligand that reflect the reactivity of these complexes as oxygen atom transfer agents.

The NMR chemical shift of the ^{17}O nucleus is affected by the electron density about oxygen and thus may be useful in assessing the susceptibility of peroxo ligands to attack by a nucleophilic substrate. Only recently have ^{17}O chemical shifts of metal-bound peroxo ligands been successfully observed. Postel examined the peroxo ligand in $MoO(O_2)(CN)_4^{2-}$;[27] Curci and Sciacovelli studied chromium, molybdenum, titanium, vanadium, and tungsten peroxo complexes with HMPA and pyridinecarboxylate ligands;[28,29] Oldfield overcame the difficulties of earlier workers in measuring the peroxo chemical shift of the O_2 adducts of Vaska's compound, $Ir(CO)X(O_2)(PPh_3)_2$ (X = Cl, I), and $Pt(O_2)(PPh_3)_2$;[30] and Herrmann reported the peroxo resonance of the diperoxorhenium complex $ReO(O_2)_2(H_2O)(CH_3)$.[31]

In this study we examine the ^{17}O peroxo chemical shifts of several previously characterized d^0 peroxo complexes. Compilation of these results with values available from the literature permits us to draw correlations among ^{17}O chemical shift, the electronic charge transfer band, the O−O vibrational frequency, and the length of the O−O bond. The relationship of these properties to reactivity is discussed.

Experimental Section

Materials. Potassium (oxalato)oxodiperoxovanadate(V), $K_3[VO(O_2)_2(C_2O_4)]\cdot nH_2O$,[32,33] potassium bis(oxalato)oxoperoxovanadate(V), $K_3[VO(O_2)(C_2O_4)_2]$,[33] and *N*-(2-hydroxyphenyl)salicylideneamine, H_2HPS,[34] were prepared by literature methods. Ammonium vanadate (Aldrich), potassium molybdate (Aldrich), potassium tungstate (Aldrich); and potassium bis(oxalato)oxotitanate(IV), $K_2[Ti(O)(C_2O_4)_2]$ (Gallard-Schlesinger), were used as received. Dioxygen gas (28 atom % ^{17}O) was obtained from Isotec. Oxygen-17-labeled hydrogen peroxide was synthesized by a modification of the method of Sitter and Terner.[35] The total hydrogen peroxide concentration of the resulting aqueous solution was typically 0.45 M. Hydrogen peroxide solutions were standardized by spectrophotometric measurement of chloroperoxidase-catalyzed triiodide formation, a modification of the method of Cotton and Dunford.[36] Carbon-13-enriched oxalate buffer (pH 5.0) was prepared from oxalic acid dihydrate (99 atom % ^{13}C, Isotec). 3-(Trimethylsilyl)propanesulfonic acid, sodium salt (DSS), was obtained from Aldrich.

NMR Spectroscopy. All spectra were acquired at 25 °C unless otherwise noted. Oxygen-17 NMR spectra were measured in 10 mm tubes on a General Electric GN-300 (7.0 T, 40.74 MHz) or GN-500 (11.7 T, 67.80 MHz) spectrometer against distilled water as the external reference (0 ppm). Spectra were acquired without a field lock. The spectral width was 143 000 Hz, and the number of accumulations ranged from 200 to 2.9×10^5. Because spin−spin relaxation of ^{17}O in peroxo complexes is extremely rapid, a short acquisition delay (10 μs) was employed in order to obtain information early in the FID.[30] For data collected on the GN-300 instrument, the severely rolling baseline resulting from pulse breakthrough was diminished by subtraction (left shift) of the first five to seven points from the FID. This correction was not required for data collected on the GN-500 spectrometer. A line-broadening factor of 50−100 Hz was applied in the exponential multiplication.

Vanadium-51 NMR spectra were measured to confirm the identity and purity of all vanadium-containing samples. Spectra were acquired in 10 mm tubes at 79.0 MHz (GN-300) or 131.5 MHz (GN-500) against $VOCl_3$ as the external reference (0 ppm). No field lock was employed. The relaxation delay was 100 ms (GN-300) or 200 ms (GN-500). The spectral width was 143 000 Hz. The number of accumulations ranged from 80 to 2000. A line-broadening factor of 20 Hz was used.

Carbon-13 NMR spectra were measured to ascertain the integrity of $MoO(O_2)_2(C_2O_4)^{2-}$ and its precursor, $MoO_3(C_2O_4)(H_2O)^{2-}$. Spectra were acquired in 5 mm tubes at 125.8 MHz (GN-500) against DSS as the external reference (0 ppm). The aqueous samples contained at least 20% ^2H_2O for the field lock. The relaxation delay was 1 s. The spectral width was 30 000 Hz. The number of accumulations ranged from 150 to 2000. A line-broadening factor of 1 Hz was used.

NMR Samples. Our examination of the ^{17}O NMR spectra of several compounds under conditions of varying ionic strength up to 1.0 M showed that the position and shape of the peroxo resonance were unaffected by change in ionic strength. Therefore, no attempt was made to maintain the same ionic strength between samples. Solutions contained a metal ion concentration of 10−30 mM and a total H_2O_2 concentration of 10−100 mM (ca. 28 atom % ^{17}O). Vanadium-51 chemical shifts, given in parentheses in the following list and measured in the solvent system indicated in Table 1 for each complex, agreed with literature values where available. The ^{17}O-labeled peroxo complexes $VO(O_2)^+$ (−544 ppm[37]), $VO(O_2)_2^-$ (−690 ppm[38]), $VO(O_2)(dipic)(H_2O)^-$ (−595 ppm,[39] dipic = pyridine-2,6-dicarboxylate), $VO(O_2)(C_2O_4)_2^{3-}$ (−596 ppm[39]), $VO(O_2)(IDA)^-$ (−588 ppm, IDA = iminodiacetate), $VO(O_2)(HPS)^-$ (−535 ppm,[40] H_2HPS = *N*-(2-hydroxyphenyl)salicylideneamine), $MoO(O_2)(dipic)(H_2O)$,[41,42] $MoO(O_2)_2(C_2O_4)^{2-}$,[17] $MoO(O_2)_2(H_2O)_2$,[25] $MoO(O_2)_2(OH)(H_2O)^-$,[25] $WO(O_2)_2(OH)(H_2O)^-$,[25] and $Ti(O_2)(C_2O_4)_2^{2-}$ [43] were prepared in situ from the appropriate ligand, buffer, metal complex (ammonium vanadate, sodium vanadate, potassium molybdate, potassium tungstate, or $K_2[TiO(C_2O_4)_2]$), and labeled hydrogen peroxide. This method minimized dilution of the ^{17}O label. The complex $VO(O_2)_2(C_2O_4)^{3-}$ (−737 ppm[39]) could not be prepared in situ from dilute (0.45 M) hydrogen peroxide and was therefore prepared from the unlabeled solid compound; enrichment was effected by exchange with $H_2{}^{17}O_2$. For the ^{13}C NMR experiments, samples of $MoO(O_2)_2(C_2O_4)^{2-}$ and $MoO_3(C_2O_4)(H_2O)^{2-}$ were prepared from potassium molybdate (40 mM) and ^{13}C-enriched oxalate buffer (pH 5.0, 80 mM); the former sample also contained H_2O_2 (120 mM).

UV/Visible and Infrared Spectroscopy. Electronic spectra of the unlabeled peroxo complexes were measured on a Hewlett-Packard 8452a diode array spectrophotometer. Infrared spectra were measured on a Nicolet 740 FTIR spectrometer. Assignments for the O−O and V=O stretches of $(NH_4)[VO(O_2)(dipic)(H_2O)]$ were made by comparison of the spectrum at natural abundance with that obtained after

(20) Bortolini, O.; Di Furia, F.; Scrimin, P.; Modena, G. *J. Mol. Catal.* **1980**, *7*, 59−74.
(21) Huston, P.; Espenson, J. H.; Bakac. A. *Inorg. Chem.* **1993**, *32*, 4517−4523.
(22) Espenson, J. H.; Pestovsky, O.; Huston, P.; Staudt, S. *J. Am. Chem. Soc.* **1994**, *116*, 2869−2877.
(23) Vassell, K. A.; Espenson, J. H. *Inorg. Chem.* **1994**, *33*, 5491−5498.
(24) Zhu, Z.; Espenson, J. H. *J. Org. Chem.* **1995**, *60*, 1326−1332.
(25) Ghiron, A. F.; Thompson, R. C. *Inorg. Chem.* **1988**, *27*, 4766−4771.
(26) Clague, M.; Butler, A. *J. Am. Chem. Soc.* **1995**, *117*, 3475−3484.
(27) Postel, M.; Brevard, C.; Arzoumanian, H.; Riess, J. G. *J. Am. Chem. Soc.* **1983**, *105*, 4922−4926.
(28) Curci, R.; Fusco, G.; Sciacovelli, O.; Troisi, L. *J. Mol. Catal.* **1985**, *32*, 251−257.
(29) Camporeale, M.; Cassidei, L.; Mello, R.; Sciacovelli, O.; Troisi, L.; Curci, R. *Stud. Org. Chem. (Amsterdam)* **1988**, *33*, 201−210.
(30) Lee, H. C.; Oldfield, E. *J. Magn. Reson.* **1986**, *69*, 367−370.
(31) Herrmann, W. A.; Fischer, R. W.; Scherer, W.; Rauch, M. U. *Angew. Chem., Int. Ed. Engl.* **1993**, *32*, 1157−1160.
(32) Vuletic, N.; Djordjevic, C. *J. Chem. Soc., Dalton Trans.* **1973**, 1137−1141.
(33) Schwendt, P.; Petrovic, P.; Uskert, D. *Z. Anorg. Allg. Chem.* **1980**, *466*, 232−236.
(34) Clague, M. J.; Keder, N. L.; Butler, A. *Inorg. Chem.* **1993**, *32*, 4754−4761.
(35) Sitter, A. J.; Terner, J. *J. Labelled Compd. Radiopharm.* **1985**, *22*, 461−465.
(36) Cotton, M. L.; Dunford, H. B. *Can. J. Chem.* **1973**, *51*, 582−587.
(37) Campbell, N. J.; Dengel, A. C.; Griffith, W. P. *Polyhedron* **1989**, *8*, 1379−1386.
(38) Literature value is −697 ppm.[37]
(39) Rehder, D.; Weidemann, C.; Duch, A.; Priebsch, W. *Inorg. Chem.* **1988**, *27*, 584−587.
(40) The chemical shift in DMF/H_2O solution is −519 ppm.[34]
(41) Jacobson, W. E.; Tang, R.; Mares, F. *Inorg. Chem.* **1978**, *17*, 3055−3063.
(42) Won, T.-J.; Sudam, B. M.; Thompson, R. C. *Inorg. Chem.* **1994**, *33*, 3804−3810.
(43) Griffith, W. P.; Wickins, T. D. *J. Chem. Soc. A* **1967**, 590−592.

Table 1. Spectroscopic and Structural Properties of Selected Peroxometal Complexes[a]

complex	buffer or solvent	δ_{O-O}, ppm ($\Delta\nu_{1/2}$, Hz)	λ_{max}, nm	ν_{O-O}, cm^{-1}	O−O bond length, Å
$VO(O_2)^+$	0.5 M $HClO_4$	**660 (1200)**[b]	**455**		
$VO(O_2)(pic)(H_2O)_2$	$CDCl_3$/MeOH	641 (4000)[c,d]	450[d]	935[e]	1.435(3)[e]
$VO(O_2)(dipic)(H_2O)^-$	acetate, pH 5.0	**608 (1700)**[b]	**432**	**910**[f]	1.441(3)[g]
	H_2O/MeCN	**610 (1600)**[h]	**424**		
$VO(O_2)(C_2O_4)_2^{3-}$	oxalate, pH 5.0	**600 (1600)**[b]	**426**	904[i]	1.430(10)[j]
$VO(O_2)(IDA)^-$	acetate, pH 5.0	**592 (1700)**[b]	**420**	920[k]	1.435(5)[k]
$VO(O_2)(HPS)^-$	MeCN/H_2O	**532 (8600)**[h]	**358**		
$Ti(O_2)(C_2O_4)_2^{2-}$	oxalate, pH 5.0	**591 (1400)**[h]	**372**		
$Ti(O_2)(dipic)(H_2O)_2$	$CDCl_3$/HMPA	585 (3200)[c,d]	400[d]	929[l]	1.464(2),[m] 1.458(2)[n]
$MoO(O_2)(dipic)(H_2O)$	MeCN	**536 (1600)**[h]	**368**	900[o]	1.447(8)[o]
$MoO(O_2)(CN)_4^{2-}$	CH_2Cl_2	487 (1800)[p]	390[q]	898[p]	1.416(5)[q]
$VO(O_2)_2^-$	acetate, pH 5.0	**444 (1000), 464 (1600)**[h]	**330**	890[r]	
$VO(O_2)_2(C_2O_4)^{3-}$	oxalate, pH 5.0	**450**[s]	**328**	875, 880, 898[t]	1.460(6), 1.451(6)[u]
$MoO(O_2)_2(H_2O)_2$	0.1 M $HClO_4$	**435 (1600)**[b]	**326**		
$MoO(O_2)_2(C_2O_4)^{2-}$	oxalate, pH 5.0	**433 (1100)**[h]	**320**	872[v]	1.480(2), 1.466(2)[w]
$MoO(O_2)_2(HMPA)$	$CDCl_3$/$CHCl_3$	468 (2000)[c,d]	320[d]	865[x]	1.498(8), 1.494(8)[y]
$MoO(O_2)_2(OH)(H_2O)^-$	acetate, pH 5.0	**412 (1700)**[b]	**310**		
$WO(O_2)_2(HMPA)$	1,2-$C_2H_4Cl_2$	400 (4100)[c,d]	245[d]	835[x]	1.51, 1.53[z]
$WO(O_2)_2(OH)(H_2O)^-$	0.1 M $HClO_4$	**346 (950), 361 (1100)**[h]	**234**		
$CrO(O_2)_2(py)$	$CDCl_3$/$CHCl_3$	726 (700), 785 (700)[c,aa]	580[bb]	934[cc]	1.407(16), 1.400(16)[dd]
$CrO(O_2)_2(HMPA)$	$CDCl_3$/$CHCl_3$	770 (890), 818 (870)[c,d]	580[d]	910, 949[ee]	
$ReO(O_2)_2(CH_3)(H_2O)$	Et_2O	363 (1250), 422 (1250)[ff,gg]	364[gg]	877[gg]	1.474(4)[gg,hh]
H_2O_2	H_2O	**178**		877,[ii,jj] 880[jj,kk]	1.49(1),[ll] 1.475(4),[mm] 1.49(2),[nn] 1.453(7)[oo]

[a] Data from this work are in boldface type; remaining data are from the references indicated. [b] Spectrometer frequency = 40.74 MHz. [c] Spectrometer frequency = 27.12 MHz. [d] Reference 29. [e] Mimoun, H.; Saussine, L.; Daire, E.; Postel, M.; Fischer, J.; Weiss, R. *J. Am. Chem. Soc.* **1983**, *105*, 3101−3110. [f] $NH_4[VO(O_2)(dipic)(H_2O)]$. [g] $NH_4[VO(O_2)(dipic)(H_2O)]\cdot 1.3H_2O$. Drew, R. E.; Einstein, F. W. B. *Inorg. Chem.* **1973**, *12*, 629−635. [h] Spectrometer frequency = 67.80 MHz. [i] $K_3[VO(O_2)(C_2O_4)_2]\cdot H_2O$. Reference 33. [j] $K_3[VO(O_2)(C_2O_4)_2]\cdot 0.5H_2O$. Stomberg, R. *Acta Chem. Scand.* **1986**, *A40*, 168−176. [k] $NH_4[VO(O_2)(IDA)]$. Djordjevic, C.; Craig, S. A.; Sinn, E. *Inorg. Chem.* **1985**, *24*, 1281−1283. [l] Mühlebach, J.; Müller, K.; Schwarzenbach, G. *Inorg. Chem.* **1970**, *9*, 2381−2390. [m] Schwarzenbach, G. *Helv. Chim. Acta* **1972**, *55*, 2990−3004. [n] Manohar, H.; Schwarzenbach, G. *Helv. Chim. Acta* **1974**, *57*, 1086−1095. [o] Reference 41. [p] $[MoO(O_2)(CN)_4][N(PPh_3)_2]_2$. Reference 27. [q] $[MoO(O_2)(CN)_4][PPh_4]_2$. Reference 63. [r] $K[VO(O_2)_2(H_2O)]$. Reference 33. [s] Signal coincides with that of $VO(O_2)_2^-$. No line width was measured. [t] $K_3[VO(O_2)_2(C_2O_4)]$. Reference 33. [u] $K_3[VO(O_2)_2(C_2O_4)]\cdot H_2O$. Begin, D.; Einstein, F. W. B.; Field, J. *Inorg. Chem.* **1975**, *14*, 1785−1790. [v] $K_2[MoO(O_2)_2(C_2O_4)]$. Dengel, A. C.; Griffith, W. P.; Powell, R. D.; Skapski, A. C. *J. Chem. Soc., Dalton Trans.* **1987**, 991−995. [w] $K_2[MoO(O_2)_2(C_2O_4)]$. Reference 50. [x] Mimoun, H.; Seree de Roch, I.; Sajus, L. *Bull. Soc. Chim. Fr.* **1969**, *5*, 1481−1492. [y] $MoO(O_2)_2(HMPA)(H_2O)$. Le Carpentier, J.-M.; Schlupp, R.; Weiss, R. *Acta Crystallogr.* **1972**, *B28*, 1278−1288. [z] $WO(O_2)_2(HMPA)(H_2O)$. Amato, G.; Arcoria, A.; Ballistreri, F. P.; Tomaselli, G. A.; Bortolini, O.; Conte, V.; Di Furia, F.; Modena, G.; Valle, G. *J. Mol. Catal.* **1986**, *37*, 165−175. [aa] Reference 28. [bb] In benzene. Evans, D. F. *J. Chem. Soc.* **1957**, 4013−4018. [cc] Reference 59. [dd] Stomberg, R. *Ark. Kemi* **1964**, *22*, 29−47. [ee] Reference 66. [ff] Spectrometer frequency = 54.21 MHz. [gg] Reference 31. [hh] Diglyme adduct. [ii] Vapor. [jj] Giguère, P. A. *J. Chem. Phys.* **1950**, *18*, 88−92. [kk] Liquid. [ll] Vapor, by electron diffraction. Giguère, P. A. *Bull. Soc. Chim. Fr.* **1954**, *21*, 720−723. [mm] Vapor, by IR. Redington, R. L.; Olson, W. B.; Cross, P. C. *J. Chem. Phys.* **1962**, *36*, 1311−1326. [nn] Solid, by X-ray diffraction. Abrahams, S. C.; Collin, R. L.; Lipscomb, W. N. *Acta Crystallogr.* **1951**, *4*, 15−20. [oo] Solid, by neutron diffraction. Busing, W. R.; Levy, H. A. *J. Chem. Phys.* **1965**, *42*, 3054−3059.

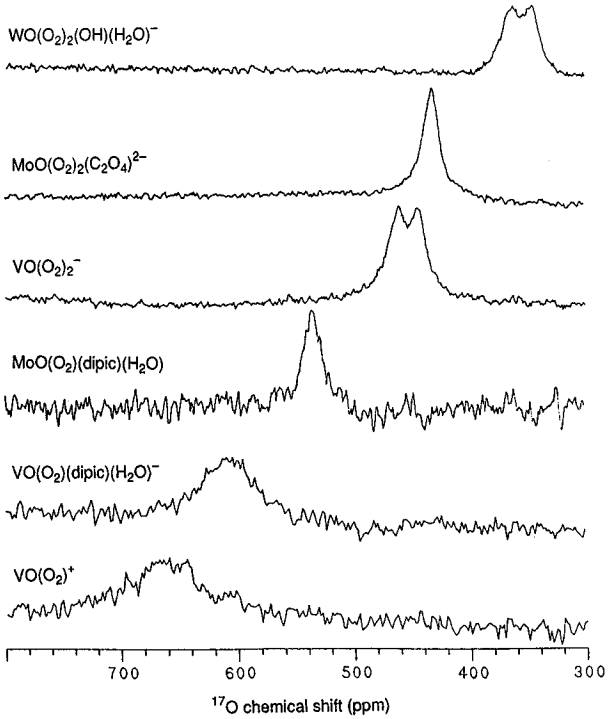

Figure 1. ^{17}O NMR spectra of several peroxo complexes. Spectra were obtained with an 11.7 T spectrometer at 67.80 MHz.

exchange of the bound peroxo group with $H_2{}^{17}O_2/H_2{}^{18}O_2$. The exchange was effected by dissolution of the solid complex in a small quantity of aqueous H_2O_2 that contained 28 atom % ^{17}O and 40 atom % ^{18}O (prepared as described above). Slow evaporation of water yielded orange-red crystals from which a KBr pellet was prepared.

Results

The metal-bound peroxo group exhibits a broad resonance in the ^{17}O NMR spectrum downfield from that of free H_2O_2 (178 ppm relative to H_2O), as displayed in Figure 1 for a series of mono- and diperoxo d^0 metal complexes prepared from ^{17}O-enriched hydrogen peroxide. The spectra of $WO(O_2)_2(OH)(H_2O)^-$ and $VO(O_2)_2(H_2O)_n^-$ exhibit two peroxo resonances. A solution of the latter complex yielded a single resonance in the ^{51}V NMR spectrum, and the chemical shifts in the ^{17}O NMR spectrum were invariant over the temperature range 15−35 °C. Table 1 summarizes the ^{17}O NMR chemical shift data for the complexes studied here and for several compounds from the literature. Also compiled in Table 1 are UV/visible λ_{max} values, O−O stretching frequencies, and O−O bond lengths. Coupling of the ^{17}O nucleus ($I = {}^5/_2$) with other nuclei is not observed because rapid quadrupolar relaxation leads to large signal widths,[44] as illustrated in Table 1 by the widths of the peroxo resonances at half-height. The ^{17}O resonance of a terminal oxo ligand falls in the range 550−1500 ppm and has a much narrower line width

(44) Rodger, C.; Sheppard, N.; McFarlane, C.; McFarlene, W. In *NMR and the Periodic Table*; Harris, R. K., Mann, B. E., Eds.; Academic: New York, 1978; Chapter 12, pp 383−419.
(45) Figgis, B. N.; Kidd, R. G.; Nyholm, R. S. *Proc. R. Soc. London, A* **1962**, *269*, 469−480.
(46) Miller, K. F.; Wentworth, R. A. D. *Inorg. Chem.* **1979**, *18*, 984−988.
(47) Heath, E.; Howarth, O. W. *J. Chem. Soc., Dalton Trans.* **1981**, 1105−1110.
(48) Conte, V.; Di Furia, F.; Modena, G.; Bortolini, O. *J. Org. Chem.* **1988**, *53*, 4581−4582.

than does that of the peroxo ligand.[27,45−48] In the present study, all peroxo complexes were prepared from ^{17}O-enriched hydrogen peroxide, and no signals due to terminal oxo ligands were observed, even in solutions that were several days old. We conclude that exchange between the peroxo and oxo ligands is insignificant. The peroxo chemical shift of the complex $VO(O_2)(dipic)(H_2O)^-$ was measured in aqueous solution at pH 5.0 (608 ppm) and in water/acetonitrile solution (610 ppm). This variation in solvent composition had very little effect on the value of the chemical shift. More noticeable was the influence of pH on chemical shift, examined for two peroxo complexes of the molybdate ion. The predominant species in 0.1 M perchloric acid is $MoO(O_2)_2(H_2O)_2$, while that at pH 5.0 is $MoO(O_2)_2(OH)(H_2O)^-$.[49] The chemical shifts were 435 and 412 ppm, respectively.

The ^{13}C NMR spectrum of $MoO(O_2)_2(C_2O_4)^{2-}$ was examined in order to verify the integrity of the complex in solution. The spectrum revealed two doublets at 169.7 ppm (J_{CC} = 74 Hz) and 167.4 ppm (J_{CC} = 74 Hz). The ^{13}C NMR spectrum of $MoO_3(C_2O_4)(H_2O)^{2-}$ exhibited a singlet at 169.6 ppm. The chemical shift of the free oxalate buffer (pH 5.0) was 175.3 ppm.

The assignment of the O−O stretch of $VO(O_2)(dipic)(H_2O)^-$ in Table 1 was determined by isotopic substitution of the peroxo oxygen atoms. Upon enrichment with ^{17}O and ^{18}O, a band at 910 cm^{-1} decreases in intensity, new bands at 897, 884, and 872 cm^{-1} appear, and a narrow band at 853 cm^{-1} is replaced by a slightly broader feature at 857 cm^{-1}. If the feature at 910 cm^{-1} is taken to be the vibration due principally to the ^{16}O−^{16}O stretch of the peroxo ligand, the stretching frequencies for the heavier isotopes can be predicted by assuming the same force constant: 897 cm^{-1} (^{16}O−^{17}O), 883 cm^{-1} (^{17}O−^{17}O), 884 cm^{-1} (^{16}O−^{18}O), 870 cm^{-1} (^{17}O−^{18}O), and 858 cm^{-1} (^{18}O−^{18}O). These estimates are virtually identical to the experimentally observed frequencies.

Discussion

With the exception of the peroxotitanium(IV) complexes, which are formulated without terminal oxo ligands, the solid-state structures of the compounds in Table 1 are consistent with the geometry typical of peroxometal complexes, namely η^2 coordination of the peroxo ligand in a plane perpendicular to the terminal oxo ligand. The equatorial plane containing the peroxo ligand(s) also contains one or more other ligands, in most cases rendering the oxygen atoms of a peroxo ligand inequivalent. This inequivalence is clearly seen in Figure 1 in the spectra of $VO(O_2)_2^-$ and $WO(O_2)_2(OH)(H_2O)^-$, each of which exhibits two peroxo-type resonances. That the former complex exhibits a singlet in the ^{51}V NMR spectrum suggests the presence of a single metal species, although a rapid equilibrium between two species cannot be ruled out. The ^{17}O NMR spectrum of $MoO(O_2)_2(C_2O_4)^{2-}$ reveals only one peroxo resonance, but the inequivalence of the oxalate carbon atoms in the ^{13}C NMR spectrum suggests that (a) the oxalate ligand is certainly bound to the metal and (b) the oxalate ligand spans an equatorial and an axial position. Such a geometry is consistent with the solid-state structure of the complex[50] and implies a formal inequivalence of the peroxo oxygen atoms of a single ligand.

Chemical environment influences the resonance frequency of a nucleus, an effect that has found enormous diagnostic use. The chemical shift δ is expressed in eq 1 as (a) the difference

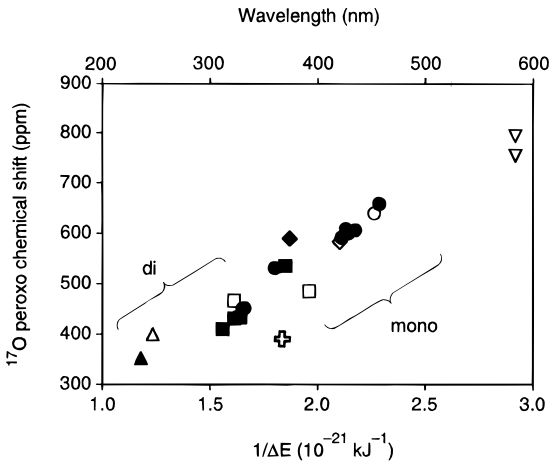

Figure 2. Plot of ^{17}O peroxo chemical shift vs the reciprocal of the LMCT energy (lower *x* axis) and wavelength (upper *x* axis) for the peroxo complexes in Table 1. Data from this work are shown as filled symbols; data from the literature are indicated by open symbols. Symbol shapes correspond to the following central metal ions: chromium (▽), molybdenum (□), rhenium (+), titanium (◇), tungsten (△), vanadium (○). Where multiple parameters are reported in Table 1, the plot employs an average value.

$$\delta = \frac{\nu - \nu_{ref}}{\nu_{ref}} \cong \sigma_{ref} - \sigma \qquad (1)$$

in resonance frequency between a particular nucleus and a reference compound and (b) the difference in shielding constant between the reference compound and the observed nucleus. Increasingly negative values of the shielding constant σ yield increasingly positive chemical shifts, and the nucleus is said to be deshielded. The shielding constant may be written as the sum of diamagnetic and paramagnetic terms, $\sigma = \sigma_d + \sigma_p$, which respectively describe the spherical and nonspherical circulation of electron density about the nucleus that is induced by the external magnetic field. For nuclei other than hydrogen, the value of σ_d changes very little with chemical environment, and shielding effects are usually described only in terms of the paramagnetic shielding parameter σ_p. A simplified form of the equation developed by Ramsey to define σ_p is shown in eq 2,

$$\sigma_p = -\frac{2e^2h^2}{3m^2c^2}\langle r^{-3}\rangle P_u(1/\Delta E) \qquad (2)$$

where $\langle r^{-3}\rangle$ is the average inverse volume and P_u is the so-called electron imbalance of a valence p orbital of the nucleus under observation, while ΔE is the average difference in energy between the ground state and all excited states of the molecule. The terms defining P_u derive from the elements of the charge density and bond order matrix, and ΔE is frequently estimated from the electronic spectrum of the molecule.[51−54]

Each of the d^0 complexes under consideration here exhibits a ligand-to-metal charge transfer (LMCT) transition in the electronic spectrum. The energy of this transition was taken to represent ΔE. A plot of δ vs $1/\Delta E$ for the complexes in Table 1 is presented in Figure 2, in which the approximately linear relationship between chemical shift and charge transfer wavelength is evident. The Ramsey equation has been invoked for correlations of this type, including that observed for a series of cobalt(III) porphyrin complexes[55] and for a set of five peroxo

(49) Lydon, J. D.; Schwane, L. M.; Thompson, R. C. *Inorg. Chem.* **1987**, *26*, 2606−2612.
(50) Djordjevic, C.; Covert, K. J.; Sinn, E. *Inorg. Chim. Acta* **1985**, *101*, L37−L39.
(51) Ramsey, N. F. *Phys. Rev.* **1950**, *78*, 699−703.
(52) Harris, R. K. *Nuclear Magnetic Resonance Spectroscopy*; Pitman: London, 1983; pp 185−193.
(53) Kintzinger, J.-P. In *Oxygen-17 and Silicon-29*; Diehl, P., Fluck, E., Kosfeld, R., Eds.; Springer-Verlag: Berlin, 1981; pp 14−20.
(54) Drago, R. S. *Physical Methods in Chemistry*; Saunders: Philadelphia, 1977; pp 282−288.

complexes containing Cr, V, Ti, Mo, and W.[29] Data for the latter complexes are included in Table 1 and Figure 2. If the Ramsey formalism and the approximation of ΔE by the charge transfer energy are indeed valid descriptions of the magnetic behavior of peroxo complexes, the fact that δ is linearly dependent on $1/\Delta E$ suggests either (a) that the properties of the peroxo oxygen orbitals represented by the values of $\langle r^{-3}\rangle$ and P_u vary relatively little across the series or (b) that these two factors vary in such a way to counterbalance each other. That $\langle r^{-3}\rangle$ and P_u should remain invariant across the range of complexes examined is quite surprising in view of the fact that the set contains metals from all three transition series, includes both mono- and diperoxo complexes, and comprises a variety of chelating ligands. In Figure 2 it is evident that mono- and diperoxo complexes segregate into two distinct groups. Monoperoxo complexes exhibit chemical shifts ranging between about 500 and 660 ppm, while the chemical shifts of diperoxo complexes run from 350 to 460 ppm. Only the complexes $CrO(O_2)_2(py)$ and $CrO(O_2)_2(HMPA)$, to be discussed later, do not fall with the other diperoxo species.

In Table 1 the expected correlation between vibrational frequency and bond length is evident: those complexes with higher O−O vibrational frequencies exhibit shorter O−O bond lengths. Monoperoxo complexes show values of ν_{O-O} above 900 cm^{-1} and O−O distances in the range 1.43−1.46 Å. Diperoxo complexes, on the other hand, have values of ν_{O-O} below 900 cm^{-1} and O−O distances of 1.46−1.53 Å, with the exception of the diperoxochromium complexes. Similar trends were noted previously for peroxovanadium(V) complexes.[5] Such effects can be understood in terms of the bonding between the peroxo ligand and the metal ion. The results of ab initio[56] and semiempirical[57] computations suggest that the metal−peroxo bonds are described by σ-interactions between the metal d_{xy} orbital and an in-plane peroxo π^* orbital, as shown in the diagram below.

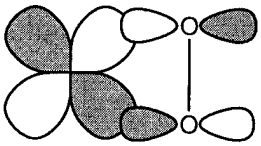

d_{xy} π^*

In a diperoxo complex, the metal $d_{x^2-y^2}$ orbital similarly interacts with a π^* orbital of a second peroxo ligand. An increasingly effective overlap of the metal and peroxo π^* orbitals should result in a diminution of electron density in the antibonding ligand orbital, increasing the strength of the O−O bonding interaction. It is reasonable to suppose that relative to the diperoxo case, in which two such ligands must compete for the metal, monoperoxo complexes exhibit an enhanced O−O interaction, apparent in the O−O stretching frequency and bond length. Examination of metal−peroxo stretching frequencies and bond distances is less instructive in this regard because of the difficulty of comparing complexes having different metal centers.

Figures 3 and 4 represent plots of O−O stretching frequency and bond length, respectively, as a function of the inverse excitation energy for the peroxo complexes in Table 1. Clear correlations are evident in both plots, suggesting that the energy

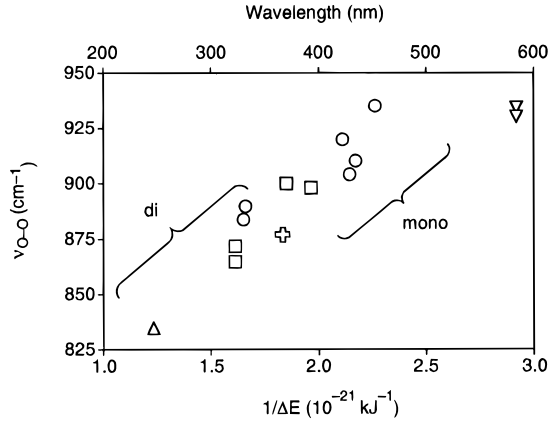

Figure 3. Plot of O−O stretching frequency vs the reciprocal of the LMCT energy (lower *x* axis) and wavelength (upper *x* axis) for the peroxo complexes in Table 1. Symbol shapes correspond to the following central metal ions: chromium (▽), molybdenum (□), rhenium (+), titanium (◇), tungsten (△), vanadium (○). Where multiple parameters are reported in Table 1, the plot employs an average value.

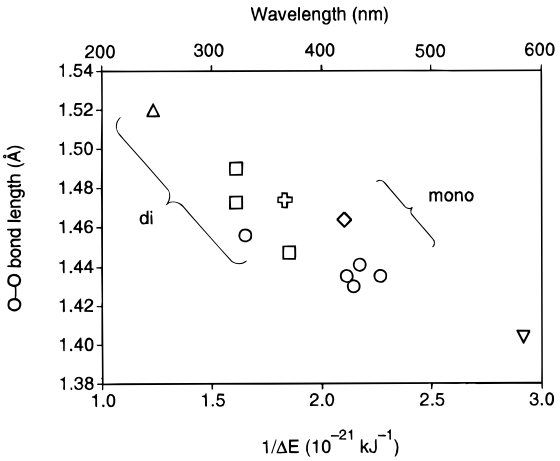

Figure 4. Plot of O−O bond length vs the reciprocal of the LMCT energy (lower *x* axis) and wavelength (upper *x* axis) for the peroxo complexes in Table 1. Symbol shapes correspond to the following central metal ions: chromium (▽), molybdenum (□), rhenium (+), titanium (◇), tungsten (△), vanadium (○). Where multiple parameters are reported in Table 1, the plot employs an average value.

of the ligand-to-metal charge transfer transition is influenced by the extent to which the peroxo π^* orbital is depleted of electron density in the peroxo−metal bonding interaction. A more complete understanding of these relationships awaits a detailed theoretical analysis of this class of complexes.

The apparently anomalous behavior of the chromium(VI) complexes was noted above. In Figures 2−4 it is evident that the diperoxochromium(VI) complexes follow the observed correlations between LMCT transition energy, chemical shift, stretching frequency, and bond length. However, the diperoxochromium(VI) ^{17}O chemical shifts lie much farther downfield, the λ_{max} values fall at significantly lower energy, the O−O bonds vibrate at higher frequencies, and the O−O bond lengths are noticeably shorter than the corresponding values of the other diperoxo complexes. A high value for the O−O stretching frequency of $CrO(O_2)_2(H_2O)$ (ν_{O-O} = 1012 cm^{-1}, resonance Raman spectrum) was attributed to π-donation to the metal from a peroxo π^* orbital orthogonal to that involved in the σ-interaction, a consequence of the high charge density of the metal.[58] Other workers noting the high values of the O−O frequency in $CrO(O_2)(py)$ and related complexes posited an interaction with the Cr═O bond.[59]

(55) Hagen, K. I.; Schwab, C. M.; Edwards, J. O.; Sweigart, D. A. *Inorg. Chem.* **1986**, *25*, 278−983.
(56) Bach, R. D.; Wolber, G. J.; Coddens, B. A. *J. Am. Chem. Soc.* **1984**, *106*, 6098−6099.
(57) Jørgensen, K. A.; Hoffmann, R. *Acta Chem. Scand.* **1986**, *B40*, 411−419.
(58) Hester, R. E.; Nour, E. M. *J. Raman Spectrosc.* **1981**, *11*, 39−42.

An early report of the infrared spectrum of $NH_4[VO(O_2)(dipic)(H_2O)]$ assigned $\nu_{O-O} = 839$ cm^{-1} and $\nu_{V=O} = 929$ cm^{-1}.[60] Another report of the spectrum of $K[VO(O_2)(dipic)(H_2O)]\cdot 2H_2O$ assigned the V=O stretch to two bands at 960 and 945 cm^{-1} but reported no features in the neighborhood of 839 cm^{-1} and indeed made no assignment for the O−O stretch.[61] Reference to Table 1 reveals that such a value for the O−O stretching frequency is anomalously low for a monoperoxovanadium complex. We were therefore prompted to determine the identity of the O−O stretch in the spectrum of $NH_4[VO(O_2)(dipic)(H_2O)]$ by isotopic substitution. It is evident that the feature at 839 cm^{-1} does not arise from the O−O stretch because no lower-frequency bands are found after substitution with heavier isotopes. Furthermore, $\nu_{O-O} = 910$ cm^{-1} is a reasonable assignment because substitution with ^{17}O and ^{18}O yields additional bands at the expected frequencies. This O−O stretching frequency is also entirely consistent with the value predicted from Figure 3 for a complex having $\lambda_{max} = 432$ nm. The earlier assignment of $\nu_{V=O} = 929$ cm^{-1} [60] is reasonable.

Several workers have reported on the relative reactivity of peroxo complexes as oxidizing agents. As noted above, the reactivity order V(V) << Mo(VI) < W(VI) for the oxidation of a cobalt-bound thiolate complex by oxo diperoxo aqua complexes illustrates the importance of the central metal in determining the activity of the metal-bound peroxo ligand.[13] Similar results for diperoxo complexes of molybdenum(VI) and tungsten(VI) in the oxidation of bromide were reported.[14,15] The effect of the number of peroxo ligands on oxidizing ability is less well defined. The monoperoxo complex $VO(O_2)(dipic)(H_2O)^-$ was several orders of magnitude slower than hydrogen peroxide in the oxidation of a coordinated thiolate ligand,[13] and both that complex[62] and $VO(O_2)(C_2O_4)_2^{2-}$ [15] oxidized bromide at pH 5.0 at a rate indistinguishable from that of hydrogen peroxide. The diperoxo complex $VO(O_2)_2^-$, by contrast, oxidized a coordinated thiolate ligand 10 times faster than did H_2O_2.[13] The monoperoxo $MoO(O_2)(dipic)(H_2O)$, while significantly more reactive than its vanadium(V) counterpart, exhibits only a fraction of the reactivity of diperoxo complexes like $MoO(O_2)_2(H_2O)_2$, $MoO(O_2)_2(OH)(H_2O)^-$, and $MoO(O_2)_2(C_2O_4)^{2-}$.[42]

These trends in reactivity are reflected in the relative positions of the peroxo complexes in the plots of Figures 2−4. In general, the more reactive complexes are those with higher-energy LMCT transitions, more shielded peroxo-group oxygen atoms, lower O−O stretching frequencies, and longer O−O bonds. Less reactive complexes are found in those areas of the plots described by lower-energy LMCT transitions, poorer shielding of peroxo-group oxygen atoms, higher O−O stretching frequencies, and shorter O−O bonds. Although the compounds in the former group are diperoxo species and monoperoxo complexes belong to the second group, Figures 2−4 suggest a reactivity continuum based on the spectroscopic properties of the complexes. The above-mentioned reactivities of diperoxo complexes of vanadium(V), molybdenum(VI), and tungsten(VI) are consistent with their relative positions in Figure 2. Furthermore, the monoperoxo complexes $MoO(O_2)(dipic)(H_2O)$[42] and $MoO(O_2)(CN)_4^{2-}$,[63] which fall near the diperoxo complexes in Figure 3, are significantly more reactive oxidizing agents than $VO(O_2)(C_2O_4)_2^{3-}$ [15] and $VO(O_2)(dipic)(H_2O)^-$,[13,62] which lie at higher O−O stretching frequencies and lower LMCT energies. This general correlation of reaction rate with the spectroscopic properties represented in Figures 2−4 suggests that the strength of the O−O bond—and therefore the ease with which it is broken—is an important factor in the reactivity of peroxo complexes.

A reverse trend was reported for one-electron oxidations by a series of vanadium(V), chromium(VI), molybdenum(VI), and tungsten(VI) peroxo complexes containing the ligands picolinate (pyridine-2-carboxylate), picolinate *N*-oxide, and benzoate. Greater oxidizing ability, as measured by increasingly positive reduction potentials from cyclic voltammetry, corresponded to an increase in O−O stretching frequency.[64] That this trend differs from the present results emphasizes the importance of distinguishing between oxidative pathways involving radicals and oxygen atom transfer.

Although the complex $VO(O_2)(HPS)^-$ has not been isolated, it was observed spectroscopically and shown to be involved in the oxidation of bromide when VO(HPS)(OEt)(EtOH) was treated with H_2O_2.[34] The values of ^{17}O chemical shift and LMCT energy for $VO(O_2)(HPS)^-$ place it in Figure 2 near $MoO(O_2)(dipic)(H_2O)$ and $MoO(O_2)(CN)_4^{2-}$, consistent with its being a relatively reactive monoperoxo complex. These examples suggest that the spectroscopic properties of peroxo complexes might be used in a general way to predict reactivity. Those complexes with the greatest reactivity have λ_{max} values smaller than 400 nm, stretching frequencies below 900 cm^{-1}, and ^{17}O chemical shifts below 600 nm. The prediction of reactivity from relatively simple spectroscopic measurements has enormous utility in the design of new catalysts, haloperoxidase analogues, and insulin mimics.

From their position in Figures 2−4 and on the basis of the trends described above, the diperoxochromium(VI) complexes are expected to be the least reactive toward substrate oxidation of the compounds under consideration here. In fact, $CrO(O_2)_2(py)$ was reported to oxidize alcohols[65] and $CrO(O_2)_2(HMPA)$ to oxidize organic sulfides.[66] The latter complex oxidized sulfides at a rate $^1/_{20}$th that of the molybdenum(VI) analogue. Kinetic studies in chloroform indicate that HMPA dissociates from the metal before the substrate is oxidized and that the actual oxidants are "free" diperoxometal species that are more reactive than their HMPA precursors.[66]

The activation of peroxide by d^0 transition metals toward the transfer of an oxygen atom to a nucleophilic substrate is often explained in terms of the increasing electrophilic character of the peroxo group by virtue of its attachment to a highly charged metal ion.[16,66] The present analysis suggests that peroxo group reactivity represents a balance between increasing electrophilicity and the increasing strength of the O−O bond that accompanies the loss of electron density from the peroxo π^* orbital.

Acknowledgment. Support of this work by NSF Research Planning Grant CHE-9309944 (M.S.R.), a Colgate University Research Council Picker Fellowship (M.S.R.), and NIH Grant GM38130 (A.B.) is gratefully acknowledged. We thank Melissa J. Clague for helpful discussions and preparation of the H_2HPS ligand.

IC951212D

(59) Fergusson, J. E.; Wilkins, E. J.; Young, J. F. *J. Chem. Soc.* **1962**, 2136−2141.
(60) Offner, F.; Dehand, J. *C. R. Hebd. Seances Acad. Sci., Ser. C* **1971**, *273*, 50−53.
(61) Wieghardt, K. *Inorg. Chem.* **1978**, *17*, 57−64 (see also Table II, supplementary material).
(62) Raebiger, J. W.; Reynolds, M. S. Unpublished results.
(63) Arzoumanian, H.; Petrignani, J. F.; Pierrot, M.; Ridouane, F.; Sanchez, J. *Inorg. Chem.* **1988**, *27*, 3377−3381.
(64) Bonchio, M.; Conte, V.; Di Furia, F.; Modena, G.; Moro, S.; Carofiglio, T.; Magno, F.; Pastore, P. *Inorg. Chem.* **1993**, *32*, 5797−5799.
(65) Fleet, G. W. J.; Little, W. *Tetrahedron Lett.* **1977**, 3749−3750.
(66) Curci, R.; Giannattasio, S.; Sciacovelli, O.; Troisi, L. *Tetrahedron* **1984**, *40*, 2763−2771.